



**HAL**  
open science

## **INTERFACIAL ADHESION OF BASALT FIBRE REINFORCED POLYMER COMPOSITES**

Maria Carolina Seghini, Fabienne Touchard, Fabrizio Sarasini, V. Cech,  
Laurence Chocinski-Arnault, David Mellier, Jacopo Tirillo, Maria Paola  
Bracciale, M. Zvonek

► **To cite this version:**

Maria Carolina Seghini, Fabienne Touchard, Fabrizio Sarasini, V. Cech, Laurence Chocinski-Arnault, et al.. INTERFACIAL ADHESION OF BASALT FIBRE REINFORCED POLYMER COMPOSITES. TWENTY-SECOND INTERNATIONAL CONFERENCE ON COMPOSITE MATERIALS (ICCM22), Aug 2019, Melbourne, Australia. hal-03008706

**HAL Id: hal-03008706**

**<https://hal.science/hal-03008706>**

Submitted on 16 Nov 2020

**HAL** is a multi-disciplinary open access archive for the deposit and dissemination of scientific research documents, whether they are published or not. The documents may come from teaching and research institutions in France or abroad, or from public or private research centers.

L'archive ouverte pluridisciplinaire **HAL**, est destinée au dépôt et à la diffusion de documents scientifiques de niveau recherche, publiés ou non, émanant des établissements d'enseignement et de recherche français ou étrangers, des laboratoires publics ou privés.

# INTERFACIAL ADHESION OF BASALT FIBRE REINFORCED POLYMER COMPOSITES

M.C. Seghini<sup>1,2,\*</sup>, F. Touchard<sup>2</sup>, F. Sarasini<sup>1</sup>, V. Cech<sup>3</sup>, L. Chocinski-Arnault<sup>2</sup>, D. Mellier<sup>2</sup>, J. Tirillo<sup>1</sup>,  
M.P. Bracciale<sup>1</sup>, M. Zvonek<sup>3</sup>

<sup>1</sup> Department of Chemical Engineering Materials Environment, Sapienza-Università di Roma, Rome, Italy

<sup>2</sup> Institut PPRIME, CNRS-ENSMA, Université de Poitiers, Département Physique et Mécanique des Matériaux, Futuroscope Cedex, France

<sup>3</sup> Institute of Materials Chemistry, Faculty of Chemistry, Brno University of Technology, Brno, Czech Republic

**Keywords :** Basalt fibres, Interface, Fibre/matrix adhesion, Fragmentation, Micro-CT analysis

## ABSTRACT

The aim of the present work is to compare the effects of a commercial coupling agent, a thermal de-sizing treatment and a plasma polymerization process on the interfacial adhesion of basalt fibres with polymer matrix. The different basalt fibres were characterized in terms of surface morphology, by FE-SEM observations, and chemical composition, performing FT-IR analysis. Fragmentation tests allowed the determination of the interfacial shear strength (IFSS) at fibre/matrix interface, while the adhesion quality was assessed in terms of critical fragment length and debonding length. The plasma polymerization process was able to produce a homogeneous tetravinylsilane (pp-TVS) coating on the surface of basalt fibres, which resulted in a significant increase in the adhesion between basalt fibre and epoxy resin. The surface roughness of the untreated and treated basalt fibres has been measured by Atomic Force Microscopy (AFM) and the results demonstrate how surface topography can play a significant role in the domain of fiber/matrix interfacial adhesion. High-resolution microtomography ( $\mu$ -CT) has been used to support the analysis of the damage mechanisms during fragmentation tests.

## 1 INTRODUCTION

In recent years, there has been substantial interest on the application of basalt fibres as reinforcement of polymer matrices. These can be proposed as a replacement for glass fibres in view of their advantages in terms of environmental cost relative to their chemical and physical properties. Basalt fibres are extruded at a temperature around 1500-1700°C from a melt of basalt rock. In particular, their similar chemical structure to glass, even though their density is slightly higher (2.8 g/cm<sup>3</sup> compared to 2.54 g/cm<sup>3</sup> of glass), makes easier its replacement. Also, the chemical stability of the basalt fibres is higher than that of glass fibres. High modulus, good strength and elastic behaviour make this kind of fibres a good alternative to the glass ones [1]. Unfortunately, the mechanical performance of a fibrous composite is not only dictated by the properties of the single constituents (fibres and matrix), but also by fibre/matrix adhesion [2]. A crucial issue for developing basalt fibres reinforced polymer composites is to analyze and optimize their interface quality. Much academia and industry efforts have gone into increasing the fibre/matrix adhesion. Several strategies have been proposed over the years in order to enhance the interfacial adhesion of basalt fibres: (i) incorporation of nanofillers into sizing formulations [3][4], (ii) bulk modification of the matrices by using coupling agents [5][6] or by nanofillers dispersion [7]. Another way to improve the performance of composites via interface engineering is the plasma-chemical process, which is considered as one of the most effective methods to optimize both strength and toughness if materials for coating and process parameters are carefully selected [8][9]. Unlike plasma treatment, which is used to increase the surface roughness and introduce functional groups into the surface layer of fibres with limited increase in interfacial shear strength [10], the plasma polymerization process is able to produce homogeneous and pinhole free films on the fibres in a clean environment without use of solvents and at low temperature, thus minimizing the risks of mechanical

properties degradation of the substrate. This process proved to be successful for glass fibres [11]–[14] but no study, to the best of authors' knowledge, is available on basalt fibres. In this work, the surface, morphological and mechanical properties of plasma-polymerized basalt fibres with a tetravinylsilane film are investigated. Plasma-polymerized organosilicones represent a class of versatile materials with a sound scientific background and their use as a tailored interlayer to improve interfacial adhesion of surface modified basalt fibres in epoxy-based composites is tested. Comparisons with commercially sized basalt fibres and basalt fibres after sizing removal are made. The adhesion to epoxy matrix is studied by single fibre fragmentation tests (SFFT).

## **2 MATERIALS AND METHODS**

### **2.1 Materials**

A commercial continuous roving of basalt fibres (Kamenny Vek), characterized by a nominal diameter of 13  $\mu\text{m}$  and by the presence of a commercial sizing optimized for epoxy resin, has been selected. Concerning the polymer resin, the epoxy Prime 27 infusion resin, supplied by Gurit, has been used for the manufacture of composite specimens.

### **2.2 Treatments**

In order to remove the commercial sizing from the basalt surface, fibre bundles were heat treated as-received in a tube furnace (Lenton Thermal Designs) at a temperature of 400°C in air for 1 h and then removed from the furnace and allowed to cool in room temperature air. After the thermal treatment, a plasma polymerized tetravinylsilane (pp-TVS) film has been deposited on the unsized basalt fibres by Plasma-Enhanced Chemical Vapor Deposition (PECVD) process. The polymer deposition treatment has been divided in two steps: a first non-polymerising gas plasma step, a pre-treatment with oxygen plasma (5.8 Pa, 100 W) for 30 min to remove contaminants, activate the fibre surface and improve film adhesion, and a second step of polymerising gas plasma, in which tetravinylsilane monomer  $\text{Si}(-\text{CH}=\text{CH}_2)_4$  was fragmented and ionized in plasma producing excited species, free radicals and ions which were recombined forming a thin plasma polymer film onto the fibre surface. Tetravinylsilane plasma (3.8 Pa, 10 W) was employed for 15 min.

### **2.3 Tensile testing**

Tensile properties of basalt fibres have been determined by single fibre tensile tests in accordance with ASTM C-1557. Tensile tests were carried out at room temperature using a Zwick/Roell Z010 machine equipped with a 100 N load cell. Each test has been performed in displacement control at a cross-head speed of 2 mm/min. Fibre diameter was evaluated through an optical microscope Nikon Eclipse 150L.

## 2.4 Single fibre fragmentation tests

According to previous works [15], the single fibre fragmentation test has been used to assess the interfacial properties of basalt fibres with epoxy matrix. Tests were performed with an Instron E1000 ElectroPuls test machine with a load cell of 2 kN, using a crosshead speed of 0.005 mm/min. The loading phase was stopped if the specimen failed, or when the fragmentation saturation level was achieved. This last case was defined when no new fibre breaks appeared during a subsequent strain increase by 0.5%. After each fragmentation test, all the fragment lengths were determined by using a ZEISS Axio Imager optical microscope. To study in a proper manner the interfacial debonding phenomena between the basalt fibre and the epoxy resin, a birefringence analysis has been performed for the untreated basalt fibre/epoxy, the thermally treated basalt fibre/epoxy and the tetravinylsilane plasma treated basalt fibre/epoxy systems. During optical microscopy observation, the fragmented single fibre composite samples were placed into a circular polariscope in order to observe the stress state near the fibre breaks and the interface between the single basalt fibre and the matrix.

## 2.5 Morphological and chemical characterization

Morphological investigations have been carried out through a field-emission gun scanning electron microscope (FE-SEM) Zeiss Auriga and a Philips XL40. The roughness of the untreated and treated basalt fibres has been measured using a Bruker Dimension Icon AFM. The chemical composition has been studied by Fourier-transform infrared (FTIR) analysis with Bruker Vertex 70 spectrometer (Bruker Optik GmbH).

# 3 RESULTS AND DISCUSSION

## 3.1 Basalt fibres characterization

At first, a morphological investigation of the lateral surfaces of the different basalt fibres have been carried out through FE-SEM. Figure 1 shows the micrographs found for the untreated and the heat-treated basalt fibres. The comparison between Figure 1-a and Figure 1-b highlights the ability of the heat treatment in removing the protective sizing layer, exposing the superficial defects present on the as received fibres. Concerning the plasma deposition process, a continuous pp-TVS film has been homogeneously deposited on all over the lateral surface of basalt fibre after the PECVD treatment. The presence of the pp-TVS film has been demonstrated by intentionally producing some scratches on the fibre surface, Figure 2.

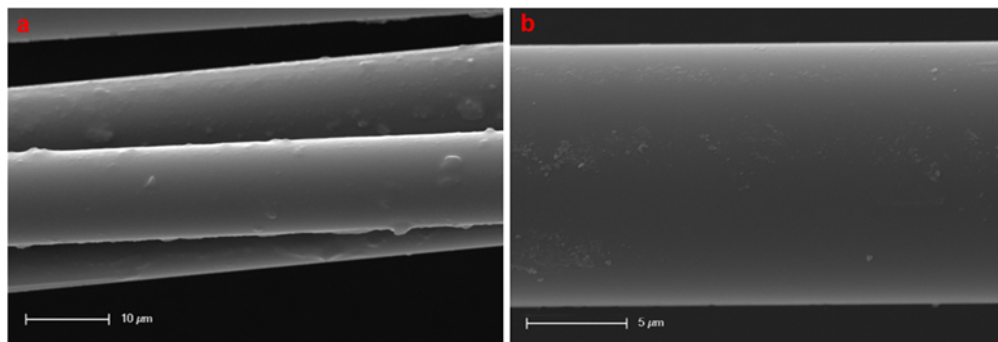


Figure 1: Scanning electron micrographs detailing the lateral surface of untreated (a) and thermally treated (b) basalt fibres.

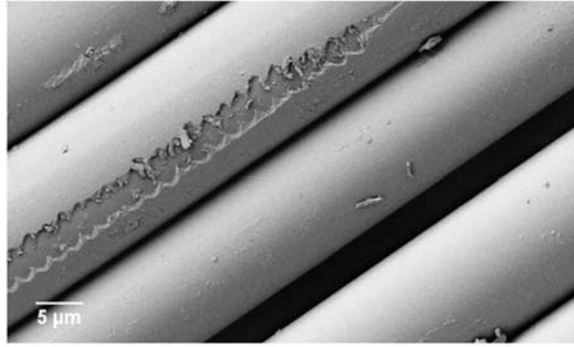


Figure 2: Scanning electron micrograph showing several uniformly plasma treated fibres and an intentionally scratched fibre.

The surface roughness of the untreated and treated basalt fibres has been measured by AFM [Seghini basalt 2019]. Differences in the surface topography of the different basalt fibres have been found. From results described in Table 1, it is possible to observe how a lower surface roughness has been found for the untreated basalt fibres, while an increase in surface roughness has been found for both thermally treated and plasma treated basalt fibres.

	Average RMS roughness [nm]
<b>As-received Basalt</b>	$3.72 \pm 0.45$
<b>Basalt 400 °C - 1h (sizing removal)</b>	$7.57 \pm 2.79$
<b>Basalt 400 °C - 1h + PECVD</b>	$7.46 \pm 2.23$

Table 1: Average RMS roughness and IFSS values for different basalt fibres.

These results indicate that the heat treatment is able to remove, at least partially, the sizing layer present in the commercial fibres, thus exposing surface defects. The chemical composition of the treated and untreated basalt fibres was investigated employing the Fourier Transform Infrared Spectroscopy. The FT-IR spectra of as-received, thermally treated and plasma treated basalt fibres are shown in Fig. 2. The spectral analysis revealed that the characteristic bands of O=C-NH of imine at 1650 cm<sup>-1</sup>, the -NH bending at 1510 cm<sup>-1</sup> and small peaks of -CH at 2852 and 2924 cm<sup>-1</sup> were visible in the as-received sample (Fig. 2a) [16]. These bands should be due to the presence of the sizing in as-received basalt fibre and it is possible to observe how they disappeared after the thermal treatment (Fig. 2b). The presence of plasma-polymerized tetravinylsilane (pp-TVS) films deposited on thermally treated basalt fibres was confirmed by FT-IR analysis. At the wavenumber range 3700-3100 cm<sup>-1</sup> a significant band of -OH occurs. Following, wide bands in the range 3100-2750 cm<sup>-1</sup> are due to vibrations of -CH<sub>2</sub> and -CH<sub>3</sub> groups. Significant bands due to C=O vibration at 1699 cm<sup>-1</sup>, C=C stretching at 1651 cm<sup>-1</sup>, -CH<sub>2</sub> scissoring at 1455 cm<sup>-1</sup> and =CH<sub>2</sub> deformation at 1418 cm<sup>-1</sup> in vinyl group can be observed. Finally, an increase in the band belonging to Si-O-Si stretching at 980 cm<sup>-1</sup> is clearly visible in plasma-coated sample [17][18].

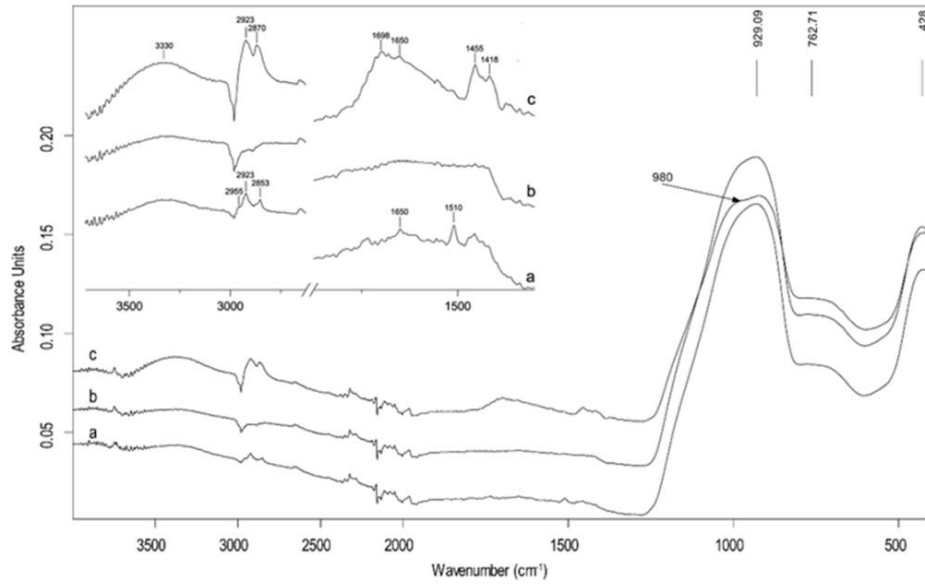


Figure 3: Infrared spectra of as-received (a), thermally treated (b) and plasma treated (c) basalt fibres.

A mechanical characterization of untreated and treated basalt fibres has been performed in order to analyze the effect of the different treatments on the tensile behavior. A comparison between the tensile results found for the commercially sized basalt fibres, the basalt fibres after the thermal sizing removal process and the plasma treated basalt fibres, is presented in Table 2. Tensile test on single fibres highlights the importance of the surface defects on the mechanical behavior of basalt fibres. In particular, a reduction and an increase in tensile strength has been found for the thermally treated and plasma treated basalt fibres, respectively. This result is clearly linked to the protective effect of the sizing agents present on the surface of the commercial basalt fibre. As highlighted by the morphological analysis, the heat treatment is able to deteriorate the protective sizing layer of the fibre, producing an exposure of the superficial defects. Zinck [19] have investigated the influence of the sizing layer on the mechanical properties of the fibres because it can fully or partially fill the surface cavities. The exposure to the plasma polymerization process after the heating treatment results in a partial recovery of the tensile properties of fibres. Comparing the results found for the thermally treated and plasma treated basalt fibres, an increase in the tensile strength has been detected after the pp-TVS film deposition. This recovery phenomenon may be ascribed to the healing effect of the pp-TVS deposited film on the surface defects of the thermally treated basalt fibres.

	Gauge Length $l_0$ [mm]	$\sigma_f$ [MPa]	$\epsilon_f$ [%]
<b>As-received Basalt</b>	20	$2515 \pm 277$	$2.41 \pm 0.32$
	30	$2440 \pm 164$	$2.6 \pm 0.24$
	40	$2410 \pm 277$	$2.5 \pm 0.4$
<b>Basalt 400 °C - 1h</b>	20	$1197 \pm 311$	$1.47 \pm 0.43$
	30	$1231 \pm 387$	$1.42 \pm 0.44$

<b>Basalt 400 °C - 1h + PECVD</b>	40	$1113 \pm 296$	$1.36 \pm 0.34$
	20	$2218 \pm 450$	$2.07 \pm 0.62$
	30	$1763 \pm 409$	$1.83 \pm 0.48$
	40	$1478 \pm 349$	$1.81 \pm 0.41$

Table 2: Summary of tensile properties of untreated and treated basalt fibres.

### 3.2 Fibre – Matrix adhesion analysis

At first, the shape of the fibre breaks inside polymer resin was analysed. This is an indicative factor of the adhesion between basalt fibre and the epoxy matrix. As reported by Kim[20], when a fibre fails and fractures earlier than the polymer matrix during the fragmentation test, the fibre ends may slip leaving empty space at the point of the fibre break. Figure 4 reports the optical micrographs found for the fragmented epoxy samples reinforced with the as-received (Fig. 4a), thermally treated (Fig. 4b) and plasma treated basalt fibres (Fig. 4c). The optical micrographs show that, for each sample, a black area corresponding with the fibre break zone has been detected. The micro-CT results confirmed that the black area found during the optical microscopy investigation corresponds to the empty zone inside the matrix produced during tensile loading. The untreated basalt fibre/epoxy samples exhibited a shape of breaks characteristic of a weak interface system, characterized by a wide breaking gap. On the contrary, both the epoxy samples reinforced with thermally treated and plasma treated basalt fibres were characterized by the presence of a reduced break gap between the fibre ends. As it is possible to see from the micrographs, Fig. 4 b-c, the epoxy matrix cracks forming a characteristic “bat-shape” break zone [21].



Figure 4: Optical micrographs of the fragmented basalt fibres: (a) as-received, (b) thermally treated and (c) plasma treated basalt fibres.

As reported by Feih [22], this shape is distinctive of a strong interface system. The birefringence method has been used to observe the interfacial debonding phenomena between the different basalt fibres and the epoxy matrix. Table 3 reports all the debonding length values found for the different specimens. Figure 5 a-b and Figure 6 a-b show the birefringence patterns found for the as received basalt fibre/epoxy system and for the single filament epoxy specimens characterized by the presence of the thermally and plasma treated basalt fibres. From Fig. 5-b it is possible to note that the maximum of the flat colour birefringence zone coincides with the black line present at the interface between the fibre and the epoxy matrix. The length of this zone has been considered for the debonding length measurement. The as-received basalt fibre/epoxy samples have shown the highest debonding length values. A symmetrical birefringence pattern has been found, Fig. 5-a, which confirms that the saturation level occurred at the end of fragmentation test. After the thermal treatment and the polymer plasma deposition process, a decrease and a lack in the flat colour zone were detected, respectively Fig. 6-a and Fig. 6-b.

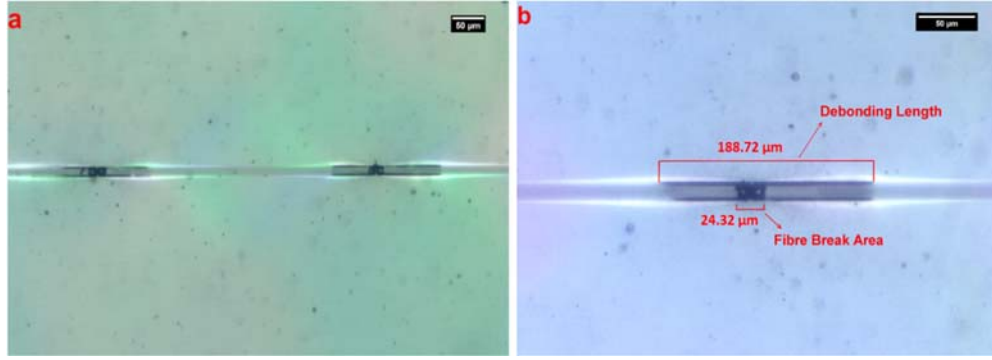


Figure 5: Optical micrograph showing the interface patterns (a) and the debonding length measurement (b) for the as-received basalt fibre/epoxy samples.

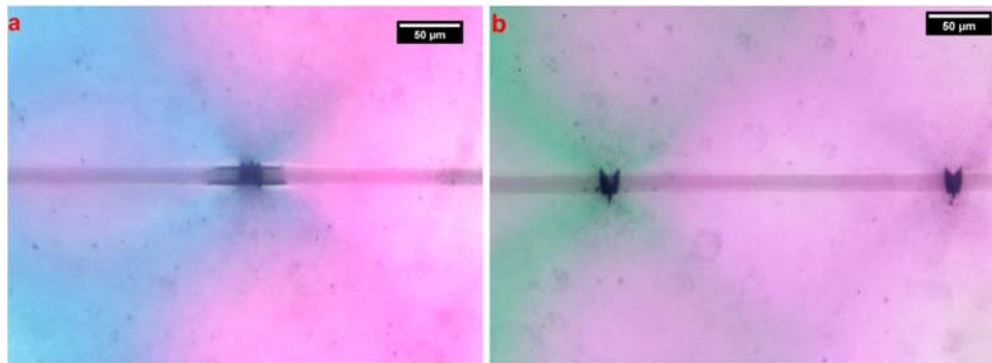


Figure 6: Optical micrograph showing the interface patterns for the thermally treated basalt fibre/epoxy (a) and the plasma treated basalt fibre/epoxy systems (b).

After the pp-TVS deposition, basalt fibres showed an increase in compatibility with the epoxy matrix evidenced by a significant reduction in the debonding phenomenon. The measurement of the critical fibre fragment length has been performed through optical microscopy. As reported by Ohsawa [23], the critical fragment length has been evaluated using equation 1:

$$l_c = \frac{4}{3} \cdot \bar{l} \quad (1)$$

where  $\bar{l}$  is the average value of the fragment length, determined as the distance between the fibre ends. According to Kelly and Tyson [24], the interfacial shear strength value (IFSS) may be estimated using equation 2:

$$IFSS = \frac{\sigma_f(l_c) \cdot d}{2 \cdot l_c} \quad (2)$$

where  $d$  is the fibre diameter,  $l_c$  is the critical fragment length and  $\sigma_f(l_c)$  is the fibre strength at a length equal to the critical fibre length. In Table 3 are reported all the critical fragment length values, the  $\sigma_f(l_c)$  values and the IFSS results obtained. The best results in terms of both critical fragment length and IFSS were found for the basalt fibres treated by the TVS plasma. From the results reported in Table 3 it may be observed that a marked increase in the values of IFSS was produced after the deposition of the polymeric film. Comparing the critical fragment lengths and the IFSS values found for the thermally

treated and the plasma treated basalt fibres, it is possible to note that the thermal treatment seems to have a positive effect on the interfacial adhesion of the basalt fibre with the epoxy matrix.

	$l_{\text{debonding}}$ [ $\mu\text{m}$ ]	$l_c$ [ $\mu\text{m}$ ]	$\sigma_f(l_c)$ [MPa]	IFSS [MPa]
<b>As-received Basalt</b>	$192.5 \pm 80$	$675.2 \pm 109$	$3591 \pm 55$	$35.4 \pm 6$
<b>Basalt 400 °C - 1h</b>	$48 \pm 8$	$353 \pm 13$	$3282 \pm 27$	$60.5 \pm 3$
<b>Basalt 400 °C - 1h + PECVD</b>	$23.5 \pm 14$	$346 \pm 48$	$3948 \pm 101$	$75.4 \pm 10$

Table 3: Debonding length, critical fragment length, and Interfacial Shear Strength of the untreated and treated basalt fibres.

Despite the sizing degradation carried out by the thermal exposure, a decrease in the critical length and an increase in the IFSS values has been produced compared to the values found for the as-received fibres. This is an interesting result because the sizing formulations are studied and optimized in order to promote the chemical bonding across the fibre/matrix interface. A possible explanation of this result may be ascribed to the increase in the surface roughness after the fibre thermal exposure that may create static frictional stresses able to affect the IFSS value.

#### 4 CONCLUSIONS

The present experimental work investigates the effects of a commercial coupling agent, a thermal de-sizing treatment and a plasma polymerization process on the fibre/matrix interfacial strength. The determination of the interfacial shear strength at fibre/matrix interface has been realized performing single fibre fragmentation tests. The study showed that the plasma deposition process is able to realize a polymeric coating able to promote the interfacial bond between the basalt fibers and the epoxy matrix. The adhesion qualities of the plasma-treated basalt fibres were found to be superior to those of commercial fibres. A reduction of the debonding and the critical fragment length as well as an increase in the value of IFSS have been obtained as a result of the pp-TVS. The study demonstrates how surface topography can play a significant role in the quality of the fiber/matrix interfacial adhesion. Indeed, an increase in the fibre surface roughness is able to promote the formation of mechanical interactions between the fibre and the polymer matrix.

#### ACKNOWLEDGEMENTS

Plasma surface modification of basalt fibers was supported by the Czech Science Foundation, grant no. 16-09161S

#### REFERENCES

- [1] V. Fiore, T. Scalici, G. Di Bella, and A. Valenza, A review on basalt fibre and its composites, *Compos. Part B Eng.*, **74**, 2015, pp. 74–94.
- [2] K. L. Pickering, M. G. A. Efendy, and T. M. Le, A review of recent developments in natural fibre composites and their mechanical performance, *Compos. - Part A*, **83**, 2016, pp. 98–112.
- [3] B. Wei, H. Cao, and S. Song, Surface modification and characterization of basalt fibers with hybrid sizings, *Compos. Part A Appl. Sci. Manuf.*, **42**, 2011, pp. 22–29.
- [4] B. Wei, S. Song, and H. Cao, Strengthening of basalt fibers with nano-SiO<sub>2</sub>-epoxy composite coating, *Mater. Des.*, **32**, 2011, pp. 4180–4186.

- [5] A. Greco, A. Maffezzoli, G. Casciaro, and F. Caretto, Mechanical properties of basalt fibers and their adhesion to polypropylene matrices, *Compos. Part B Eng.*, **67**, 2014, pp. 233–238.
- [6] F. Sarasini, J. Tirillò, C. Sergi, M. C. Seghini, L. Cozzarini, and N. Graupner, Effect of basalt fibre hybridisation and sizing removal on mechanical and thermal properties of hemp fibre reinforced HDPE composites, *Compos. Struct.*, **188**, 2018, pp. 394–406.
- [7] S. O. Lee, S. H. Choi, S. H. Kwon, K. Y. Rhee, and S. J. Park, Modification of surface functionality of multi-walled carbon nanotubes on fracture toughness of basalt fiber-reinforced composites, *Compos. Part B Eng.*, **79**, 2015, pp. 47–52.
- [8] Z. Liu, F. Zhao, and F. R. Jones, Optimising the interfacial response of glass fibre composites with a functional nanoscale plasma polymer coating, *Compos. Sci. Technol.*, **68**, 2008, pp. 3161–3170.
- [9] J.-K. Kim and Y.-W. Mai, High strength, high fracture toughness fibre composites with interface control - A review, *Compos. Sci. Technol.*, **41**, 1991, pp. 333–378.
- [10] M. T. Kim, M. H. Kim, K. Y. Rhee, and S. J. Park, Study on an oxygen plasma treatment of a basalt fiber and its effect on the interlaminar fracture property of basalt /epoxy woven composites, *Compos. Part B*, **42**, 2011, pp. 499–504.
- [11] D. J. Marks and F. R. Jones, Plasma polymerised coatings for engineered interfaces for enhanced composite performance, *Compos. Part A Appl. Sci. Manuf.*, **33**, 2002, pp. 1293–1302.
- [12] V. Cech, A. Knob, T. Lasota, J. Lukes, and L. T. Drzal, Surface modification of glass fibers by oxidized plasma coatings to improve interfacial shear strength in GF/polyester composites, *Polym. Compos.*, **40**, pp. 1–8, 2017.
- [13] V. Cech *et al.*, Enhanced interfacial adhesion of glass fibers by tetravinylsilane plasma modification, *Compos. PART A*, **58**, 2014, pp. 84–89.
- [14] V. Cech, R. Prikryl, R. Balkova, J. Vanek, and A. Grycova, The influence of surface modifications of glass on glass fiber/polyester interphase properties, *J. Adhes. Sci. Technol.*, **17**, 2003, pp. 1299–1320.
- [15] M. C. Seghini, F. Touchard, F. Sarasini, L. Chocinski-arnault, D. Mellier, and J. Tirillò, Interfacial adhesion assessment in flax/epoxy and in flax/vinylester composites by single yarn fragmentation test : Correlation with micro-CT analysis, *Compos. Part A*, **113**, 2018, pp. 66–75.
- [16] J. Kim, P. Seidler, L. S. Wan, and C. Fill, Formation, structure, and reactivity of amino-terminated organic films on silicon substrates, *J. Colloid Interface Sci.*, **329**, 2009, pp. 114–119.
- [17] V. Cech, J. Studynka, F. Janos, and V. Perina, Influence of oxygen on the chemical structure of plasma polymer films deposited from a mixture of tetravinylsilane and oxygen gas, *Plasma Process. Polym.*, **4**, 2007, pp. S776–S780.
- [18] G. Davidson, The vibrational spectrum of tetravinylsilane, *Spectrochim. Acta Part A Mol. Spectrosc.*, **27A**, 1971, pp. 1161–1169.
- [19] P. Zinck, M. F. Pays, R. Rezakhanlou, and J. F. Gerard, Mechanical characterisation of glass fibres as an indirect analysis of the effect of surface treatment, *J. Mater. Sci.*, **34**, 1999, pp. 2121–2133.
- [20] B. W. Kim and J. a Nairn, Observations of Fiber Fracture and Interfacial Debonding Phenomena Using the Fragmentation Test in Single Fiber Composites, *J. Compos. Mater.*, **36**, 2002, pp. 1825–1858.
- [21] C. L. Schutte, W. Mcdonough, M. Shioya, M. Mcauliffe, and M. Greenwood, The use of a single-fibre fragmentation test to study environmental durability of interfaces / interphases between DGEBA / mPDA epoxy and glass fibre : the effect of moisture, *Composites*, **25**, 1994 , pp. 617–624.
- [22] S. Feih, K. Wonsyld, D. Minzari, P. Westermann, and H. Lilholt, Testing procedure for the single fiber fragmentation test, *Risoe Natl. Lab.*, pp. 1–30, 2004.

- [23] T. Ohsawa, A. Nakayama, M. Miwa, and A. Hasegawa, Temperature dependence of critical fiber length for glass fiber - reinforced thermosetting resins, *J. Appl. Polym. Sci.*, **22**, 1978, pp. 3203–3212.
- [24] A. Kelly and W. R. Tyson, Tensile properties of fibre-reinforced metals: Copper/Tungsten and Copper/Molybdenum, *J. Mech. Phys. Solids*, **13**, 1965, pp. 329–350.